International Journal of Engineering Trends and Technology
ISSN: 2231–5381 / https://doi.org/10.14445/22315381/IJETT-V72I1P116

Volume 72 Issue 1, 164-173, January 2024

Original Article

A Numerical Modeling Approach to Study the Characteristics of a Photovoltaic Cell Featuring a GaAs Absorber Layer

Jhilirani Nayak[1], Priyabrata Pattanaik[2], Dilip Kumar Mishra[3]

[1,2,3]*Faculty of Engineering and Technology (ITER), Siksha 'O' Anusandhan Deemed to be University, Odisha, India.*

[1]*Corresponding Author : jhiliraninayak@soa.ac.in*

Received: 11 September 2023 Revised: 11 December 2023 Accepted: 11 December 2023 Published: 07 January 2024

Abstract *- This article provides an innovative way of constructing a Si/GaAs solar cell and investigating its electrical parameters and the electrical properties of the materials integrated into the cell. The device architecture incorporates a gallium arsenide (GaAs) emitter on the top of a silicon wafer, coated with a dual coating of zinc oxide (ZnO) and silicon dioxide (SiO2) on its surface. To enhance the overall performance of the photovoltaic device, a detailed investigation of critical parameters, including material thickness, bandgap characteristics, band alignment, and emitter carrier concentration, was conducted. The model's validity was evaluated through the performance metrics (efficiency), fill factor, and spectral response, all executed with the assistance of the COMSOL Multiphysics tool. The device exhibits a power conversion efficiency of 14.46%, a device short-circuit current of 16.401mA, and a fill factor of 0.8728. This study projects the distinctive characteristics of the device with and without the incorporation of anti-reflection coatings and its overall performance.*

Keywords *- Anti-reflection coatings, COMSOL Multiphysics, Zinc Oxide, Si/GaAs solar cell, Silicon dioxide.*

1. Introduction

In the current days, photovoltaic (PV) modules are substantially used to enhance sustainable energy generation in the global green energy market. These modules are now in high demand since they are utilised to deliver electrical power [1, 2] to a wide range of applications. Solar cell production has expanded to meet demand, and its modules are constructed by connecting solar cells to each other. One of the most crucial problems for producing affordable and competitive photovoltaic (PV) systems is accelerating power conversion performances [2].

Renewable energy is attractive due to its derivation from environmentally benign sources, which contrasts sharply with conventional production systems reliant on environmentally detrimental fossil fuels [1]. Photovoltaic cells stand as an optimal choice for clean, reliable, and inexhaustible renewable energy generation. Each day, the sun delivers an astounding 4000 quadrillion kilowatt-hours (kWh) of energy to earth [2]. Upon entering the earth's atmosphere, approximately 26 percent of incident sunlight is subjected to reflection, scattering, and dispersion through the cloud cover and atmospheric components. This solar radiation, comprised of high-energy photons, when interacting with objects, imparts energy to the electrons within the material, potentially liberating them from their bound states.

The energized electrons move from the negative terminal to the positive terminal, leading to the generation of a photovoltaic effect. This photovoltaic effect is achieved as the absorbed photons surpass the material's bandgap. Different semiconductors with different bandgaps are used to design photovoltaic cells, and the bandgaps increase as wavelength increases [1, 3].

Consequently, the photovoltaic phenomenon is absent at certain wavelengths or in specific chemical compositions [1]. Back in 1839, Becquerel discerned the photovoltaic attributes in certain compounds [4]. It was not until 1940 that the photovoltaic effect was officially identified. Over time, there has been a progressive enhancement in the power generation capacity of photovoltaic cells. With an increase in the thickness of silicon photovoltaic cells, there is typically a corresponding escalation in both their efficiency and cost. As a result, the industry has witnessed the production of photovoltaic cells with thickness variations spanning from 200 to 400 micrometers.

This strategic use of thinner materials over time has been instrumental in achieving improved cost-effectiveness and enhanced performance. Due to their inherent characteristics of thinness, brittleness, and susceptibility to oxidation, silicon cells are fashioned into panel configurations [1].

Two primary factors contributing to the degradation of solar panel efficiency are the accumulation of particulate matter and undesirable light reflection. The significant disparity in refractive indices between silicon (Si) and air results in the reflection of approximately 36% of incident light from the polished surface of a silicon wafer[5,6].The use of anti-reflection coating on the silicon surface decreases its reflectance and increases the efficiency of the silicon solar cell. Anti Reflection Coatings (ARCs) find extensive applications in diverse fields, encompassing display panels, optical lenses, and photovoltaic cells [7-9]. Through the strategic implementation of phase transitions and capitalizing on the correlation between reflectivity and refractive index, thin-film ARCs offer a substantial reduction in optical losses.

To diminish the reflectivity of an optical surface and thereby augment its transmittance, thin dielectric films or multiple analogous layers have been employed. Typically, a specific wavelength is assigned for a single-layer anti-reflection coating, frequently situated in the middle of the visible spectrum, as non-reflective [10].

In comparison to single-layer coatings, multiple-layer anti-reflection coatings demonstrate superior efficiency across the entire visible spectrum. These multilayer coatings incorporate a variety of transparent, high-refractive-index materials, including SiO (n = 1.8–1.9), SiO_2 (n = 1.44), Si_3N_4 (n = 1.9), TiO_2 (n = 2.3), Al_2O_3 (n = 1.86), Ta_2O_5 (n=2.26), and SiO_2–TiO_2 (n=1.8–1.9) [13-18], as effective means to reduce reflectance.

Recent advancements in solar cell production have led to the development and utilization of Si_3N_4 or TiO_2 single-layer coatings, characterized by both high refractive indices and excellent transparency, along with SiO_2/TiO_2 double-layer coatings.

These highly regarded coatings are synthesized through the PECVD process, resulting in reflectance levels of less than 10% [13,14,19]. By incorporating additional layers, it becomes possible to reduce reflections at specific wavelengths further. Kern and Tracy observed a notable 44 percent enhancement in cell efficiency following the application of a TiO_2 single-layer ARC [17]. In another study, Green et al. achieved a 19.1 percent efficiency in Si cells by employing MgF_2/ZnS double-layer ARCs [18]. Silicon photovoltaic cells equipped with a single anti-reflection coating layer exhibit pronounced optical losses across a broad spectrum of solar wavelengths. Double-layer anti-reflection coatings (DLARCs) are employed to enhance the photovoltaic cell's efficiency. The purpose of DLARCs is to decrease reflectance in the visible and near-infrared portions of the sunlight spectrum in order to enhance carrier collection[20-23]. Due to dual surface passivation and anti-reflection capabilities, a double-layer anti-reflection coating like SiO_2/TiO_2 or SiO_2/SiO_x is helpful in increasing efficiency.

In their research, Doshi et al. conducted simulations and optimized the ARC film thickness and refractive indices, ultimately utilizing the SiO_2/SiN_x DLARC design [22]. It is worth noting that in most ARC modeling experiments, the achieved maximum power conversion efficiency typically ranged from 3 to 13 percent [21-24].

Ayad et al. [25] conducted a study examining the impact of photon conversion on the properties of single-crystalline silicon solar cells. The results indicated a significant improvement of about 9% in the short-circuit photocurrent density, accompanied by an increase in the efficiency of converting light into electricity in silicon solar cells.

McIntosh et al. explored the influence of a luminous downshifting layer on the external quantum efficiency of enclosed silicon solar cells. At the same time, Yang and Yang examined the internal quantum efficiency and light-trapping capability of a silicon photovoltaic cell with a grating structure[27]. The three most crucial elements that affect a mono-silicon photovoltaic cell's efficiency are the temperature, total irradiance, and spectral dispersion of irradiance. [28, 29].

The spectral response of silicon solar cells stands as a pivotal characteristic. Evaluating spectral response involves the use of spectrally pure light spanning a wide wavelength range, aligning with the solar energy spectrum. For mono-Si solar cells, the acceptable wavelength range typically falls within 350-1100 nm [30]. However, generalizing the impact of solar spectrum variations on diverse solar device performances remains challenging due to the intricacies associated with spectral response measurement [31].

Another widely employed metric to convey a solar cell's sensitivity is external quantum efficiency, often referred to as quantum efficiency [11]. In an ideal photovoltaic cell, incoming photons initiate the generation of hole-electron pairs, with all photo carriers migrating towards depleted regions for subsequent separation and collection. Photocarriers cannot be produced by photons possessing energies below the material's band gap energy. Furthermore, even if they are generated, their contribution to the photocurrent is negligible [30, 32].

In the current research, a silicon-based gallium arsenide (GaAs) photovoltaic cell equipped with Zinc oxide /Silicon dioxide anti-reflection coatings has been designed and subjected to electrical property simulations. The device was simulated, yielding an efficiency of 14.6%, a fill factor of 87.28% and a short circuit current of 16.401 mA. This examined device incorporates a DLARC on a gallium arsenide solar cell featuring a surface area of 1 cm^2. The simulation-based methodology introduced in this study stands as a distinctive approach for characterizing the device with ARC layers aimed at enhancing solar cell efficiency.

This simulation technique offers a substantial reduction in both time and costs associated with the analysis of solar cells equipped with double-layer anti-reflection coatings. Additionally, it assists in the optimization of the design parameters for the anti-reflection coating layer.

2. Simulation Details of the Device

In this study, a one-dimensional COMSOL Multiphysics Simulator is employed to perform simulations. The structure of the GaAs solar cell is illustrated in Figure 1. The simulation revolves around the SiO2/ZnO/GaAs/Si heterostructure as the core device configuration. Specifically, the structure features an n-type GaAs layer chosen as the heterojunction partner, serving as the absorber layer where photogenerated charge carriers are collected. The optical properties of the model were analyzed using the Lambert-Beer model.

The simulation process adopts the standard Air Mass (AM) 1.5 as the incident light spectrum, as illustrated in Figure 2. Subsequently, the current-voltage (J-V) characteristic of the device is obtained. Furthermore, considerations were made for the series and shunt resistances, expressed in ohms, respectively. The simulator uses fundamental semiconductor equations such as the equation for continuity, the current equation for charge carriers and Poisson's equation to derive the electrical characteristics of the device.

Different physics-based models like Shockely-Read–Hall (SRH), Trap-assisted and Auger recombination were used to calculate the mobility of carriers and radiative and nonradiative recombination in cells. Finally, the COMSOL MULTIPHYSICS tool was used to get the solution of the steady-state equations and continuity equations and also to calculate device parameters.

The lattice constants of GaAs and Si differ significantly due to which, a significant lattice mismatch between the different layers.It results in a Misfit Displacement (MDs) or Threading Dislocation (TD) [33-39].

These threading dislocations spread into the photoactive cell area of the solar cell and reduce carrier lifetime by lowering the quality of the materials and diffusion length [37-38].Actually, dislocations generate a significant number of centres for recombination in the cell, lowering the overall cell performance of our device by reducing both open-circuit voltages (V_{oc}) and short-circuit current (I_{sc}) as given in the literature [33-39].

The simulation research was carried out by considering different parameters, including variations in the thickness of the layers, bandgap of the absorber GaAs and carrier concentration of GaAs–absorber. The influence of band alignment and interfaces on the proposed device is also investigated in this work.

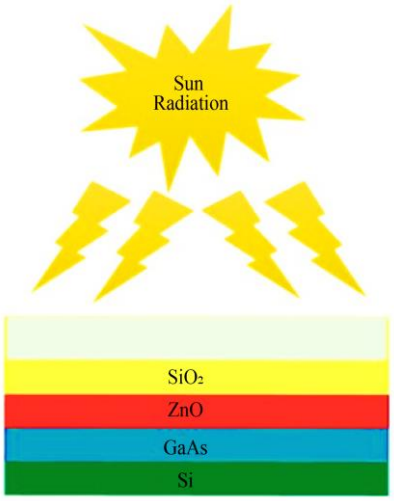

Fig. 1 Device structure of the GaAs solar cell

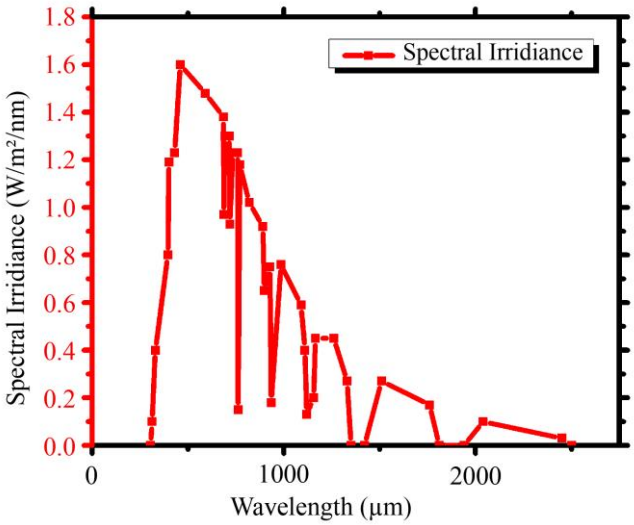

Fig. 2 The spectrum of solar radiation AM 1.5G on the surface of the earth

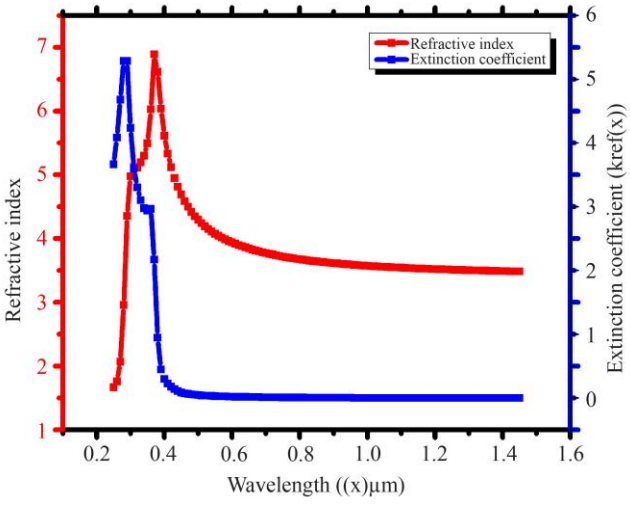

Fig. 3 Complex Refractive index of silicon

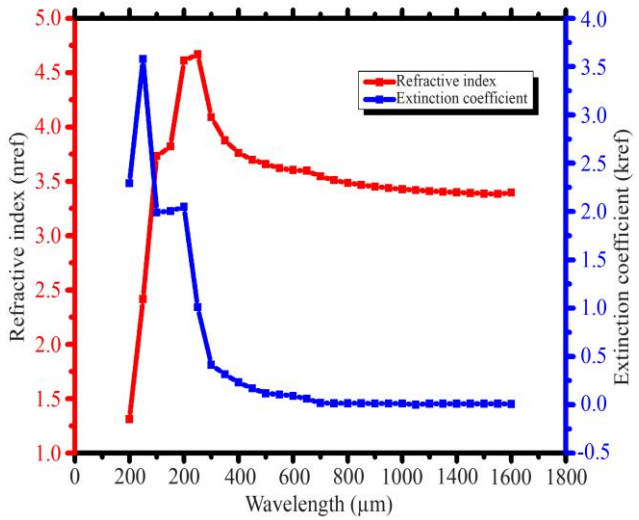

Fig. 4 Complex refractive index of GaAs

Figures 3 and 4 illustrate a graph of the complicated refractive index derived from various literature publications and databases [40–44].

3. Results and Discussion

To validate the simulation results, a comparative study and analysis of the device with double-layer anti-reflection coating was conducted. Then, it is validated with the different single ARC layer and double ARC layer devices in published articles, as presented in Table 1 [45,46,22,6,49]. The validation is done with respect to the current, voltage, fill factor and conversion efficiency. The analysis employed under the AM1.5G global spectrum is characterized by a solar irradiance of 1000 watts per square meter (W/m²), as depicted in Figure 2. It is worth noting that this spectral power distribution may undergo variations in intensity at different wavelengths based on location, weather conditions, and atmospheric absorption [50].

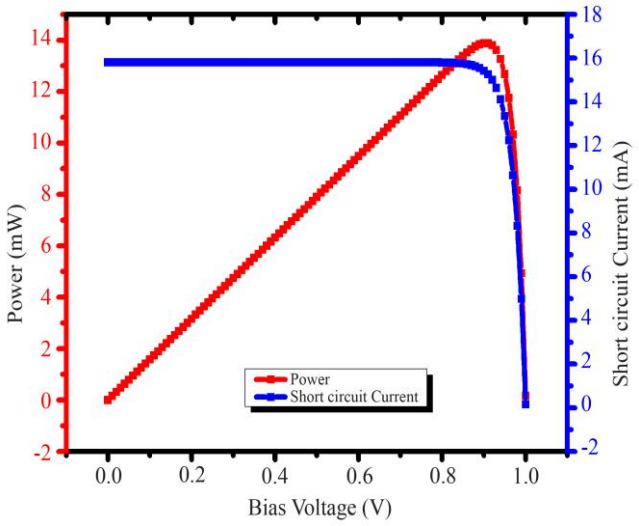

Fig. 5 I-V and P-V characteristics of the proposed photovoltaic cell

On an average day, approximately 10^{17} photons per second impinge upon a 1 cm² surface area. The estimation of critical photovoltaic cell parameters, including External Quantum Efficiency (EQE), Open-Circuit Voltage (Voc), Short-Circuit Current Density (Jsc), Conversion Efficiency (Eff), and Fill Factor (FF), was conducted using the COMSOL semiconductor tool. The intensity intricately influences these parameters or the amount of incident solar irradiance penetrating the photovoltaic cell. Given the utilization of diverse materials in the proposed device, it exhibits distinct optical and electrical characteristics. Consequently, the optical intensity within each layer of the device exhibits variations. The fluctuations observed in V_{oc} [30] can be mathematically expressed as part of the analysis

$$.V'_{OC} = \frac{nKT}{q} \ln\left[\frac{(I_L+I')}{I_O} + 1\right] \quad = X.V_{OC} \qquad (1)$$

Fig-5 shows the current-bias voltage (I-V) and power–bias voltage (P-V) characteristics of the proposed device.

3.1. Effect of Thickness of Active Layers

The active base layer thickness plays a vital role in determining an individual cell's current and voltage. As demonstrated in Fig-6, thickness alternation demonstrates an impact on the cell's Efficiency (Eff) and Short-circuit Current Density (Isc) values. In Figure 6, it is observed that the variation in efficiency, short-circuit current density, fill factor, and open-circuit voltage within our device.

The thickness of the absorber layer (GaAs) is adjusted across a range spanning from 20µm to 300µm. Within this range, significant alterations in both efficiency and short-circuit current density were evident in response to changes in the device's thickness. Simultaneously, as the thickness increased, there was a corresponding rise in the open-circuit voltage.

The graph in Figure-6(a) illustrates the variation in short-circuit current (Isc) with respect to the active layer thickness. Notably, the maximum short circuit current, recorded at 30µm layer thickness, gradually declined as the thickness increased. The proposed solar cell exhibited a peak power conversion efficiency of 14.6%, as depicted in Figure 6 (a). However, as thickness increased, the efficiency began to decrease, primarily due to the elevated bandgap. It is essential to note that photons with energy exceeding the bandgap energy of the material can initiate electron excitation and facilitate electricity generation. When photons possessing 1.8eV energy interact with the 1.5eV bandgap of the proposed cell, the excess energy (0.3eV) becomes dissipated. So, the increase in bandgap produces fewer electrons which have too much energy to contribute towards the efficiency. The open circuit voltage (Voc) shown in Figure-6(b) varies from 0.561V to 0.598V, with the variation of active layer thickness from 20µm to 300µm. Voc remains constant for a certain period and then gradually increases with the increase in layer thickness.

Table 1. Validation table

Solar Cell Model	Spectrum	Methods	Voc(V)	Isc(mA)	FF	Conversion Efficiency (%)
Rafal Pietruszka et al.[45]	AM1.5G	ZnO/Si	0.49	28.3	0.65	9.1
M.Z.Pakhuruddin et al.[46]	AM1.5	ZnO/Si (Thin film)	0.39	7.14	0.52	1.65
Galib Hashmi et al.[22]	AM1.5G	SiO_2/Si_3N_4 ARC	0.68	3.53	0.84	20.42
		SiO2/Si_3N_4 ARC & surface passivation	0.68	3.57	0.84	20.67
Sahoo et al.[6]	AM1.5G	Si_3N_4 SLAR	0.59	30.8	0.64	11.7
		Si_3N_4 SWS	0.59	33.7	0.64	12.86
Bilyalov et al.[49]	AM1.5	PS on textured	0.60	30.7	0.77	14.2
		Substrate	0.60	30.3	0.77	14.1
Proposed model	AM1.5G	SiO_2/ ZnO ARC	1.01	16.4	0.87	14.46

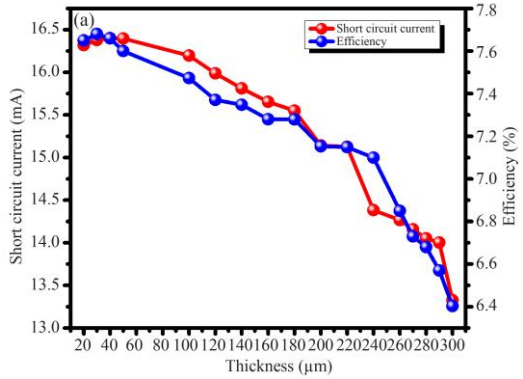

Fig. 6(a) Impact on I_{sc} & η due to variation of thickness of the top active layer of the cell

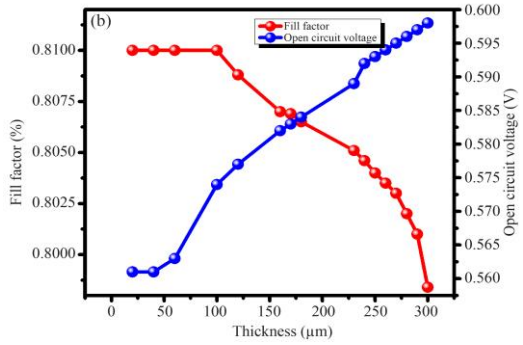

Fig. 6(b) Impact on FF & Voc due to variation of thickness of the top active layer of the cell

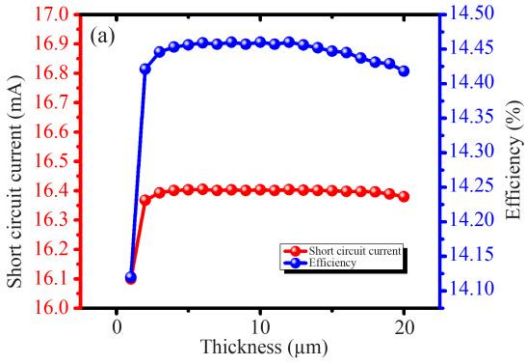

Fig. 7(a) Impact on I_{sc} & η due to variation of thickness of the bottom layer (Silicon)of the cell

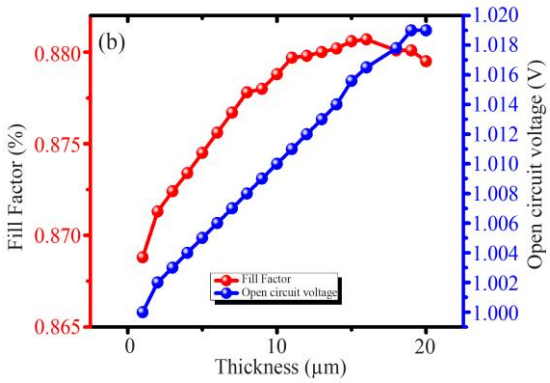

Fig. 7(b) Impact on FF & Voc due to variation of thickness of the bottom layer (Silicon)of the cell

It is less affected by the layer thickness in comparison to other parameters. The real Voc is the same as the potential built-in or contact difference. There is a little variation in the fill factor; at 300μm, the fill factor becomes 0.8858. As shown in Figure-6(b), the fill factor decreases from 0.81 to 0.7984. This decrease is due to the increase in open circuit voltage. In Figure 7, the graph illustrates how cell performance varies with the variation in silicon wafer thickness in the proposed photovoltaic model. The thickness of the silicon wafer was systematically adjusted within the range of 1μm to 20μm. Within this range, both the conversion efficiency and the current density of the device exhibited only marginal changes up to a thickness of 20μm.

Notably, Fig. 7(a) shows an enhancement in the short circuit current (I_{sc}) at 1μm thickness, followed by a relatively insignificant decrease. Remarkably, an optimum efficiency of 14.46% was achieved at a thickness of 8μm, as depicted in Figure 7 (a). However, it is observed that the increase in thickness of the base layer reduces the conversion efficiency and increases the open-circuit voltage.

Furthermore, Fig.7(b) indicates that with the silicon layer's thickness growth, both the open-circuit voltage and fill factor gradually increase. Notably, at a thickness of 20μm, the open-circuit voltage reaches 1.019V, while the fill factor reaches 87.95%. As a result, a decision was made to maintain the thickness of the top base at 30μm for subsequent analyses.

3.2. Effect of Band Alignment

In the 1970s and 1980s, the concepts were developed for band alignment of almost all of the fundamental heterojunction models. The band alignment is necessary for two ideal semiconductors to operate properly at their bulk properties [51]. The anticipated band gap and electron affinity (EA) values are crucial for the materials employed in simulating the heterojunction device structure, facilitating the efficient charge transport process across the junction. Figure 8 visually represents the band alignment and electron affinity diagram of the proposed device. It is imperative to emphasize that, in the context of constructing a solar cell, a comprehensive understanding of the energy gap between the maxima of the valence band (VBM) and the minima of the conduction band (CBM) is of paramount importance[51]. In the proposed device, a wide band gap anti-reflection layer, i.e., ZnO of 3.3eV and SiO2 of 9eV, was used to reduce reflection losses. Due to this, there is a reduction in the performance of the cell. Materials with high band gaps behave as an insulator. Positive and negative spikes occur due to the conduction band offset value at the junctions. Increased spike and cliff levels at the heterojunction may result in lower Voc and Isc. As a consequence, the heterojunction contact should be kept to a bare minimum for an efficient solar cell.

3.3. Effect of Bandgap

In this part, the analysis is based on the effect of bandgap on solar cell performance. Figure 9 depicts the variation of the device parameters corresponding to the different values of bandgap.

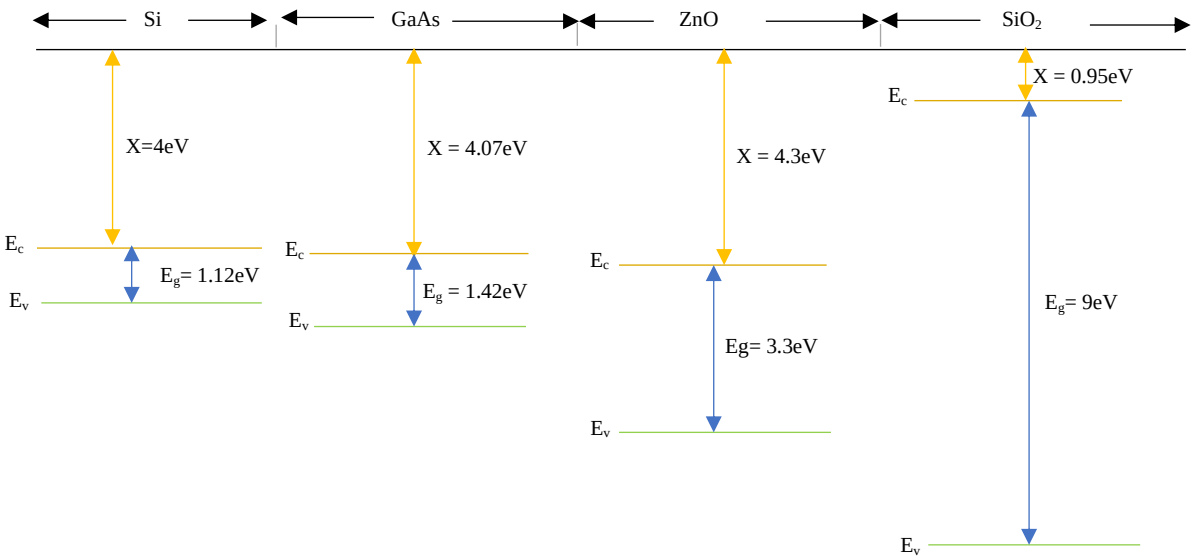

Fig. 8 Band diagram for proposed solar cell given in Fig. 1

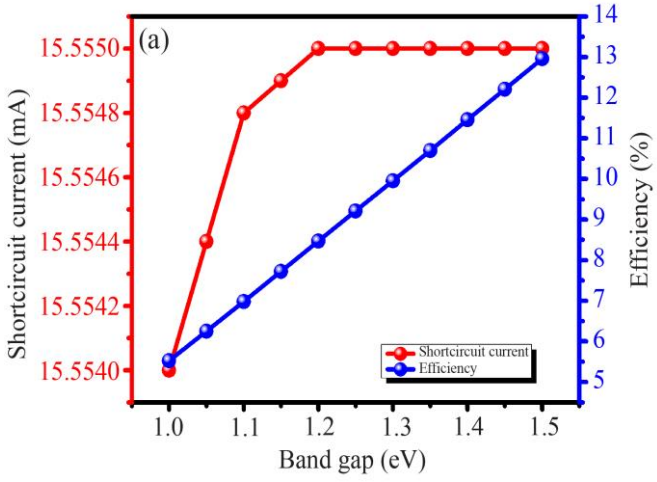

Fig. 9(a) Impact on Isc & η due to variation of the band gap of the cell

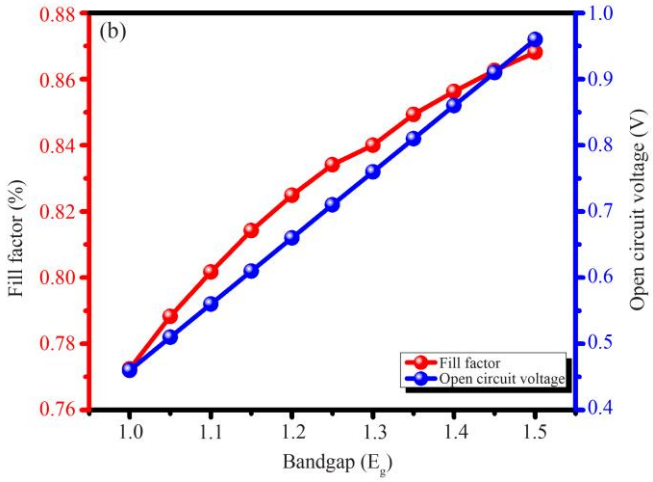

Fig. 9(b) Impact on FF & Voc due to variation of band gap of the cell

Performance variation due to bandgap variation is shown in Figure 9. The variation of short-circuit current is much less in comparison to other parameters with the variation of the bandgap. It is observed that the short circuit current changes from 15.554V to 15.555V within a bandgap variation of 1.0V to 1.2eV and remains unaltered, as shown in Figure 8 (a). The device provides better results at higher bandgaps in comparison to lower bandgaps. This is because higher energy photons are absorbed and lead to the generation of more electron-hole pairs, thus increasing the potential for higher short-circuit current and efficiency.

Figure 8 (b) indicates that V_{oc} ranges from 0.46V to .96V with the bandgap variation from 1eV to 1.5eV of the top active layer. An open circuit voltage of 0.96V with respect to a band gap of 1.5eV was observed. The fill factor in Figure-9(b) increases with an increase in band gap and ranges from 77.24% to 86.81% within the bandgap range of 1eV to 1.5eV. Looking at the effectiveness dependency on the bandgap, the efficiency of the device increases linearly. Efficiency in Figure-9(a) shows a maximum value of 12.964% over a range of 1eV to 1.5eV of bandgap.

3.4. Effect of Carrier Concentration

In this section, an investigation is conducted into the influence of carrier concentration within the absorber layer on the device parameters, as illustrated in Figure 10. As observed in Figure 10, the carrier concentration of the GaAs layer varies, ranging from 10^{17} cm^{-3} to 10^{19} cm^{-3}. Notably, the utilization of GaAs led to an increase in the open-circuit voltage (Voc), spanning from 0.87V to 1.05V. It's important to highlight that GaAs exhibit enhanced performance when their thickness is increased and the carrier concentration surpasses 10^{19} cm^{-3}. To achieve a higher Voc, the carrier concentration (N_A) should exceed 10^{17} cm^{-3}, as depicted in Figure 10(b). Figure 10(a) illustrates that the short-circuit current (Isc) remains relatively constant with an increase in carrier concentration.This constancy is attributed to the equilibrium established between carrier generation and recombination, ensuring that the dark current remains consistent. Notably, the contour graph underscores that I_{sc} exhibits a lesser dependency on the absorber layer's carrier concentration and is more influenced by the growth of the thickness of the absorber layer. However, with a further rise in doping density, I_{sc} experiences a decline. The reduction in I_{sc} is attributed to the decreasing lifespan and diffusion constant of minority charge carriers as carrier doping concentration rises, ultimately leading to a decrease in minority carrier concentration. Due to this, diffusion duration reduces, which eventually reduces the photocurrent. On the other side, reduced minority carrier concentration increases the open-circuit voltage. When electrons and holes pass continuously, they cross a given distance throughout their lifetime, known as the period of diffusion L. As a result, diffusion length is a key factor for controlling solar cell performance.

The conversion efficiency of the proposed GaAs solar cell decreases progressively with increased thickness and increases gradually with an increase in carrier concentration to a specified value of 10^{17} cm^3, respectively. For increased doping, the concentration of carrier doping grows more.

As a result, it is determined by the range of doping being investigated as well as the thickness of the absorber layer. Figure 10 (b) indicates that FF increases as the doping concentration increases. Mathematically, the fill factor can be expressed as a function r_s and r_{sh} in [30] is given by

$$FF = FF_0(1 - r_s) \quad (2)$$

$$FF = FF_0\left(1 - \frac{1}{r_{sh}}\right) \quad (3)$$

r_s is the normalized series resistance, and r_{sh} is the normalized shunt resistance of the proposed device. In the absence of parasitic resistances, FF_0 is the ideal fill factor.

$$r_s = \frac{R_s}{R_{ch}} \quad (4)$$

$$r_{sh} = \frac{R_{sh}}{R_{ch}} \quad (5)$$

The fill factor increases as the shunt resistance increases and series resistance decreases, as expressed in equations (2) and (3). As a result, series resistance decreases by increasing the fill factor. The presence of SiO_2 and ZnO leads to the existence of leakage current in the device. But its amount is less and it contributes towards a high value of shunt resistance.

A high shunt resistance value also increases the fill factor. Increasing the fill factor enhances the power conversion efficiency of the designed solar cell. The proposed device results from an enhanced fill factor. It can be controlled by a short-circuit current.

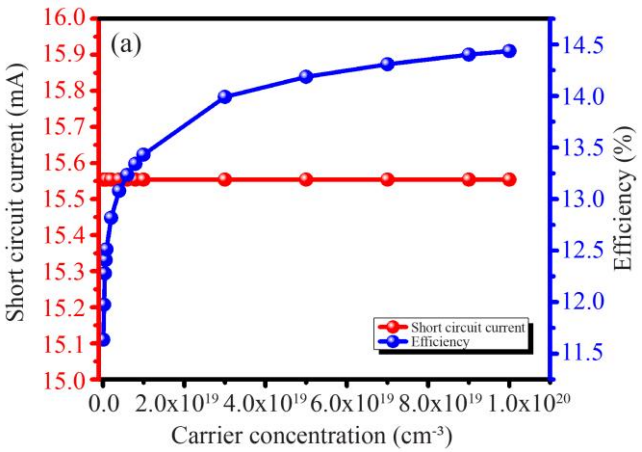

Fig. 10(a) Impact on I_{sc} & η due to variation of carrier concentration of the cell

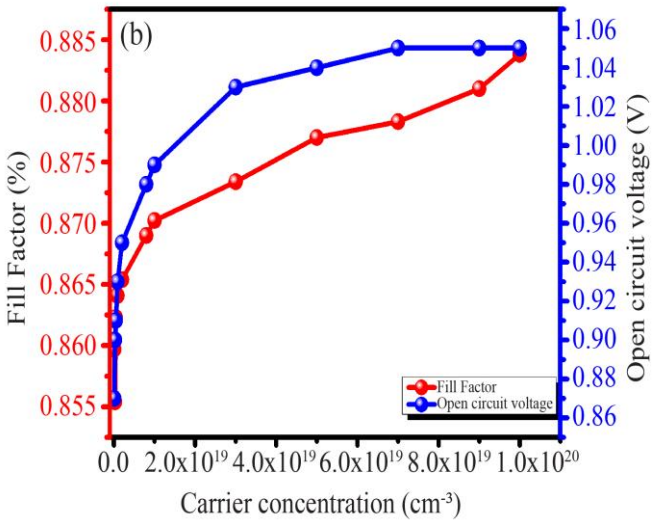

Fig. 10(b) Impact on FF & Voc due to variation of carrier concentration of the cell

4. Conclusion

This study has implemented a silicon-based GaAs solar cell model with SiO_2 and ZnO anti-reflection coatings, achieving an impressive efficiency of 14.46%. This efficiency is more incomparison to the previously referenced devices with single anti-reflection coating layers [45, 6, 4]. The device's performance trade-off can be attributed to an unoptimized band-alignment structure. It is clear from the simulation result that electrical characteristics can be improved by using a spike-type band alignment. This paper represents a thorough evaluation and comparison study on a number of cell characteristics, including conversion efficiency, fill factor, open-circuit voltage, and short-circuit current density. The results of the study show that wider bandgaps are advantageous for a number of important factors, including higher photogenerated current, better spectrum responsiveness, and higher efficiency. Furthermore, the broader bandgap arrangement has a commensurate impact on the cell's open-circuit voltage.

References

[1] Ali Samet Sarkın, Nazmi Ekren, and Şafak Sağlam, "A Review of Anti-Reflection and Self-Cleaning Coatings on Photovoltaic Panels," *Solar Energy*, vol. 199, pp. 63-73, 2020. [CrossRef] [Google Scholar] [Publisher Link]

[2] Duy Phong Pham, Sunhwa Lee, and Junsin Yi, "Optimisation of Four-Terminal GaAs//Si Tandem Solar Cells Using Numerical Simulation," *Materials Science in Semiconductor Processing*, vol. 139, 2022. [CrossRef] [Google Scholar] [Publisher Link]

[3] Rolf Brendel, *Thin-Film Crystalline Silicon Solar Cells, Physics and Technology*, Wiley-VCH Verlag GmbH and Co. KGaA, 2003. [CrossRef] [Google Scholar] [Publisher Link]

[4] Soteris A. Kalogirou, "Solar Thermal Collectors and Applications," *Progress in Energy and Combustion Science*, vol. 30, no. 3, pp. 231-295, 2004. [CrossRef] [Google Scholar] [Publisher Link]

[5] Hamdy K. Elminir et al., "Effect of Dust on the Transparent Cover of Solar Collectors," *Energy Conversion and Management*, vol. 47, no. 18-19, pp. 3192-3203, 2006. [CrossRef] [Google Scholar] [Publisher Link]

[6] Kartika Chandra Sahoo, Yiming Li, and Edward Yi Chang, "Shape Effect of Silicon Nitride Subwavelength Structure on Reflectance for Silicon Solar Cells," *IEEE Transactions on Electron Devices*, vol. 57, no. 10, pp. 2427-2433, 2010. [CrossRef] [Google Scholar] [Publisher Link]

[7] D. Bouhafs et al., "Design and Simulation of Antireflection Coating Systems for Optoelectronic Devices: Application to Silicon Solar Cells," *Solar Energy Materials and Solar Cells*, vol. 52, no. 1-2, pp. 79-93, 1998. [CrossRef] [Google Scholar] [Publisher Link]

[8] Anthony Yen et al., "An Anti-Reflection Coating for Use with PMMA at 193 nm," *Journal of the Electrochemical Society*, vol. 139, no. 2, 1992. [CrossRef] [Google Scholar] [Publisher Link]

[9] J. Sczybowski et al., "Large-Scale Antireflective Coatings on Glass Produced by Reactive Magnetron Sputtering," *Surface and Coatings Technology*, vol. 98, no. 1-3, pp. 1460-1466, 1998. [CrossRef] [Google Scholar] [Publisher Link]

[10] Shui-Yang Lien et al., "Tri-layer Antireflection Coatings (Sio2/Sio2–Tio2/Tio2) for Silicon Solar Cells Using a Sol–Gel Technique," *Solar Energy Materials and Solar Cells*, vol. 90, no. 16, pp. 2710-2719, 2006. [CrossRef] [Google Scholar] [Publisher Link]

[11] Subhash Chander et al., "A Study on Spectral Response and External Quantum Efficiency of Mono-Crystalline Silicon Solar Cell," *International Journal of Renewable Energy Research*, vol. 5, no. 1, pp. 41-44, 2015. [Google Scholar] [Publisher Link]

[12] Maruthamuthu Subramanian et al., "Optimization of Antireflection Coating Design Using PC1D Simulation for C−Si Solar Cell Application," *Electronics*, vol. 10, no. 24, pp. 1-11, 2021. [CrossRef] [Google Scholar] [Publisher Link]

[13] C. Martinet et al., "Deposition of SiO2 and TiO2 Thin Films by Plasma Enhanced Chemical Vapor Deposition for Antireflection Coating," *Non-Crystalline Solids*, vol. 216, pp. 77-82, 1997. [CrossRef] [Google Scholar] [Publisher Link]

[14] H. Nagel, A. Metz, and R. Hezel, "Porous SiO2 Films Prepared by Remote Plasma-Enhanced Chemical Vapour Deposition – A Novel Antireflection Coating Technology for Photovoltaic Modules," *Solar Energy Materials and Solar Cells*, vol. 65, no. 1-4, pp. 71-77, 2001. [CrossRef] [Google Scholar] [Publisher Link]

[15] A. Morales, and A. Duran, "Sol-Gel Protection of Front Surface Silver and Aluminum Mirrors," *Journal of Sol-Gel Science and Technology*, vol. 8, pp. 451-457, 1997. [CrossRef] [Google Scholar] [Publisher Link]

[16] T. Schuler, and M.A. Aegerter, "Optical, Electrical and Structural Properties of Sol Gel ZnO: Al Coatings," *Thin Solid Films*, vol. 351, no. 1-2, pp. 125-131, 1999. [CrossRef] [Google Scholar] [Publisher Link]

[17] W. Kern, and E. Tracy, "Titanium Dioxide Antireflection Coating For Silicon Solar Cells by Spray Deposition," *RCA Rev*, vol. 41, pp. 133-180, 1980. [Google Scholar] [Publisher Link]

[18] M.A. Green et al., "19.1% Efficient Silicon Solar Cell," *Applied Physics Letters*, vol. 44, pp. 1163-1164, 1984. [CrossRef] [Google Scholar] [Publisher Link]

[19] I.O. Parm et al., "High-Density Inductively Coupled Plasma Chemical Vapor Deposition of Silicon Nitride for Solar Cell Application," *Solar Energy Materials and Solar Cells*, vol. 74, no. 1-4, pp. 97-105, 2002. [CrossRef] [Google Scholar] [Publisher Link]

[20] Parag Doshi, Gerald E. Jellison, and Ajeet Rohatgi, "Characterization and Optimization of Absorbing Plasma-Enhanced Chemical Vapor Deposited Antireflection Coatings for Silicon Photovoltaics," *Applied Optics*, vol. 36, no. 30, pp. 7826-7837, 1997. [CrossRef] [Google Scholar] [Publisher Link]

[21] A. Lennie et al., "Modelling and Simulation of SiO/Si N as Anti-Reflecting Coating for Silicon Solar Cell by Using Silvaco Software," *World Applied Sciences Journal*, vol. 11, no. 7, pp. 786-790, 2010. [Google Scholar] [Publisher Link]

[22] Galib Hashmi et al., "Investigation of the Impact of Diferent ARC Layers Using PC1D Simulation: Application to Crystalline Silicon Solar Cells," *Journal of Theoretical and Applied Physics*, vol. 12, pp. 327-334, 2018. [CrossRef] [Google Scholar] [Publisher Link]

[23] Rajinder Sharma, "Silicon Nitride as Antireflection Coating to Enhance the Conversion Efficiency of Silicon Solar Cells," *Turkish Journal of Physics*, vol. 42, no. 4, pp. 350-355, 2018. [CrossRef] [Google Scholar] [Publisher Link]

[24] D.N. Wright, E.S. Marstein, and A. Holt, "Double Layer Anti-Reflective Coatings for Silicon Solar Cells," *Conference Record of the Thirty-first IEEE Photovoltaic Specialists Conference*, Lake Buena Vista, FL, USA, pp. 1237–1240, 2005. [CrossRef] [Google Scholar] [Publisher Link]

[25] Mohammed Ayad et al., "Studies of the Effect of a Photons Converter (LDS) on the Characteristic Parameters of the Solar Cells," *International Journal of Renewable Energy Research*, vol. 2, no. 4, pp. 596-599, 2012. [Google Scholar] [Publisher Link]

[26] Keith R. McIntosh et al., "Increase in External Quantum Efficiency of Encapsulated Silicon Solar Cells from a Luminescent Down-Shifting Layer," *Progress in Photovoltaics: Research and Applications*, vol. 17, no. 3, pp. 191-197, 2009. [CrossRef] [Google Scholar] [Publisher Link]

[27] Kuo-Hui Yang, and Jaw-Yen Yang, "The Analysis of Light Trapping and Internal Quantum Efficiency of a Solar Cell with Grating Structure," *Solar Energy*, vol. 85, no. 3, pp. 419-431, 2011. [CrossRef] [Google Scholar] [Publisher Link]

[28] Libin Zeng et al., "A Simplified Method to Modulate Colors on Industrial Multicrystalline Silicon Solar Cells with Reduced Current Losses," *Solar Energy*, vol. 103, pp. 343-349, 2014. [CrossRef] [Google Scholar] [Publisher Link]

[29] Sanjeev K. Sharma et al., "Review on Se-and S-Doped Hydrogenated Amorphous Silicon Thin Films," *Indian Journal of Pure and Applied Physics*, vol. 52, no. 5, pp. 293-313, 2014. [Google Scholar] [Publisher Link]

[30] Chetan Singh Solanki, *Solar Photovoltaics, Technology and Systems, A Manual for Technicians, Trainers and Engineers*, PHI Learning, pp. 1-320, 2013. [Google Scholar] [Publisher Link]

[31] G. Nofuentes et al., "Analysis of the Dependence of the Spectral Factor of Some PV Technologies on the Solar Spectrum Distribution," *Applied Energy*, vol. 113, pp. 302-309, 2014. [CrossRef] [Google Scholar] [Publisher Link]

[32] L. Fang, L. Danos, and T. Markvart, "Solar Cell as a Waveguide: Quantum Efficiency of Ultrathin Crystalline Silicon Solar Cell," *Proceedings of the 28th European Photovoltaic Solar Energy Conference and Exhibition*, Paris, France pp. 31-33, 2013. [CrossRef] [Google Scholar] [Publisher Link]

[33] Kevin Nay Yaung et al., "GaAsP Solar Cells on GaP/Si with Low Threading Dislocation Density," *Applied Physics Letters*, vol. 109, pp. 1-9, 2016. [CrossRef] [Google Scholar] [Publisher Link]

[34] Michelle Vaisman et al., "GaAs Solar Cells on V-Grooved Silicon via Selective Area Growth," *2017 IEEE 44th Photovoltaic Specialist Conference (PVSC)*, Washington, DC, USA, pp. 578-581, 2017. [CrossRef] [Google Scholar] [Publisher Link]

[35] Nikhil Jain, and Mantu K. Hudait, "Impact of Threading Dislocations on the Design of GaAs and InGaP/GaAs Solar Cells on Si Using Finite Element Analysis," *IEEE Journal of Photovoltaics*, vol. 3, no. 1, pp. 528-534, 2013. [CrossRef] [Google Scholar] [Publisher Link]

[36] John F. Geisz et al., "Generalized Optoelectronic Model of Series-Connected Multijunction Solar Cells," *IEEE Journal of Photovoltaics*, vol. 5, no. 6, pp. 1827-1839, 2015. [CrossRef] [Google Scholar] [Publisher Link]

[37] S.A. Ringel et al., "Single-Junction InGaP/GaAs Solar Cells Grown on Si Substrates with SiGe Buffer Layers," *Progress in Photovoltaics: Research and Applications*, vol. 10, no. 6, pp. 417-426, 2002. [CrossRef] [Google Scholar] [Publisher Link]

[38] Masafumi Yamaguchi, Akio Yamamoto, and Yoshio Itoh, "Effect of Dislocations on the Efficiency of Thin-Film Gaas Solar Cells on Si Substrates," *Journal of Applied Physics*, vol. 59, pp. 1751-1753, 1986. [CrossRef] [Google Scholar] [Publisher Link]

[39] Han Zhang et al., "Evaluating the Effect of Dislocation on the Photovoltaic Performance of Metamorphic Tandem Solar Cells," *Science China Technological Sciences*, vol. 53, pp. 2569-2574, 2010. [CrossRef] [Google Scholar] [Publisher Link]

[40] Robert E. Morrison, "Reflectivity and Optical Constants of Indium Arsenide, Indium Antimonide, and Gallium Arsenide," *Physical Review*, vol. 124, no. 5, 1961. [CrossRef] [Google Scholar] [Publisher Link]

[41] D.E. Aspnes et al., "Optical Properties of $Al_xGa_{1-x}AS$," *Journal of Applied Physics*, vol. 60, pp. 754-767, 1986. [CrossRef] [Google Scholar] [Publisher Link]

[42] Sadao Adachi et al., "Refractive Index of $(Al_xGa_{1-x})_{0.5}In_{0.5}P$ Quaternary Alloys," *Journal of Applied Physics*, vol. 75, pp. 478-480, 1994. [CrossRef] [Google Scholar] [Publisher Link]

[43] Hirokazu Kato et al., "Optical Properties of $(Al_xGa_{1-x})_{0.5}In_{0.5}P$ Quaternary Alloys," *Japanese Journal of Applied Physics*, vol. 33, 1994. [CrossRef] [Google Scholar] [Publisher Link]

[44] D.E. Aspnes, and A.A. Studna, "Dielectric Functions and Optical Parameters of Si, Ge, GaP, GaAs, GaSb, InP, InAs, and InSb from 1.5 to 6.0 eV," *Physical Review B*, vol. 27, no. 2, 1983. [CrossRef] [Google Scholar] [Publisher Link]

[45] Rafal Pietruszka et al., "9.1% Efficient Zinc Oxide/Silicon Solar Cells on a 50 μm Thick Si Absorber," *Beilstein Journal of Nanotechnology*, vol. 12, pp. 766-774, 2021. [CrossRef] [Google Scholar] [Publisher Link]

[46] M.Z. Pakhuruddin et al., "Fabrication and Characterization of Zinc Oxide Anti-Reflective Coating on Flexible Thin Film Microcrystalline Silicon Solar Cell," *Optik*, vol. 124, no. 22, pp. 5397–5400, 2013. [CrossRef] [Google Scholar] [Publisher Link]

[47] Galib Hashmi et al., "Investigation of the Impact of Diferent ARC Layers Using PC1D Simulation: Application to Crystalline Silicon Solar Cells," *Journal of Theoretical and Applied Physics*, vol. 12, pp. 327–334, 2018. [CrossRef] [Google Scholar] [Publisher Link]

[48] Muchen Sui, Yuxin Chu, and Ran Zhang, "A Review of Technologies for High Efficiency Silicon Solar Cells," *Journal of Physics: Conference Series*, vol. 1907, 2021. [CrossRef] [Google Scholar] [Publisher Link]

[49] Renat R. Bilyalov et al., "Use of Porous Silicon Antireflection Coating in Multicrystalline Silicon Solar Cell Processing," *IEEE Transactions on Electron Devices*, vol. 46, no. 10, pp. 2035-2040, 1999. [CrossRef] [Google Scholar] [Publisher Link]

[50] Alexander P. Kirk, *Solar Photovoltaic Cells Photons to Electricity*, Elsevier Science, pp. 1-138, 2014. [Google Scholar] [Publisher Link]

[51] Sadanand, and D.K. Dwivedi, "Modeling of Photovoltaic Solar Cell Based on $CuSbS_2$ Absorber for the Enhancement of Performance," *IEEE Transactions on Electron Devices*, vol. 68, no. 3, pp. 1121-1128, 2021. [CrossRef] [Google Scholar] [Publisher Link]